# TUBE STRESSES DUE TO IN-PLANE THERMAL EXPANSION OF TUBESHEETS IN CLOSELY SPACED DOUBLE TUBESHEETS†

Alan I. Soler
Chief Technology Officer
Holtec International

*ABSTRACT*

*An approximate analysis of thermal stresses developed in heat exchanger tubing between closely spaced double tubesheets is presented. Tube loading is caused by in-plane differential thermal movement of the adjacent tubesheets. To obtain solutions valid for arbitrary spacing between the tubesheets, the effect of shear deformation is included. The effect of edge restraint such as peripheral flange bolting is also included. Typical results are presented to illustrate the interaction of bending and shear in the tubes.*

## INTRODUCTION

Preventing fluid leakage between shell side and tube side of shell and tube heat exchangers, due to tube joint leakage, is of prime importance in the design of units where intermingling of component fluids is undesirable. One method of eliminating shell and tubeside fluid leakage involves using double tubesheet construction. In double tubesheet construction, a loading of particular importance, which may be the governing condition in establishing minimum tubesheet spacing, is a differential movement of the adjacent tubesheets in their own plane due to tubesheet heating. The in-plane thermal movements of the closely spaced tubesheets induce bending and shearing actions in the tubing between the tubesheets; the tubesheet spacing must be set so as to maintain the maximum tube stress below some design level under the most severe tubesheet differential movements. Reference 1 presents a simple, but

† This work was sponsored by Ecolaire Condenser, Inc., Lehigh Valley, Pa.



*Int. J. Pres. Ves. & Piping* (7) (1979)—
Printed in Great Britain

conservative, estimate of the required gap between tubesheets due to the thermal effect by assuming that the tube is built-in at each tubesheet and that the tube accommodates differential lateral end movement (due to tubesheet heating) by bending action only. Ignoring any elastic effects of the tubesheets, reference 1 gives a conservative estimate of the relationship between tubesheet spacing $L$ and the thermal loading parameter $\Delta_T$ as:

$$a\Delta_T = \frac{\sigma_a L^2}{3Ed_T} \tag{1}$$

where: $E$ = Young's modulus of tube; $d_T$ = tube outer diameter; $\sigma_a$ = design stress level in tube bending and $\Delta_T = |(\alpha_T T_T - \alpha_s T_s)|$.

In the above $\Delta_T$ represents unrestrained differential in-plane thermal movements between tubesheets that induce tube flexure, $\alpha_i$ are thermal expansion coefficients of the tubesheet materials and $T_i$ are tubesheet temperature changes from the assembly temperature. The length, $a$, is the characteristic length over which unrestrained expansion occurs.

In Fig. 1, which shows a typical double tubesheet configuration, eqn. (1) applies only if the spacing $L$ between tubesheets is large enough so that interaction between

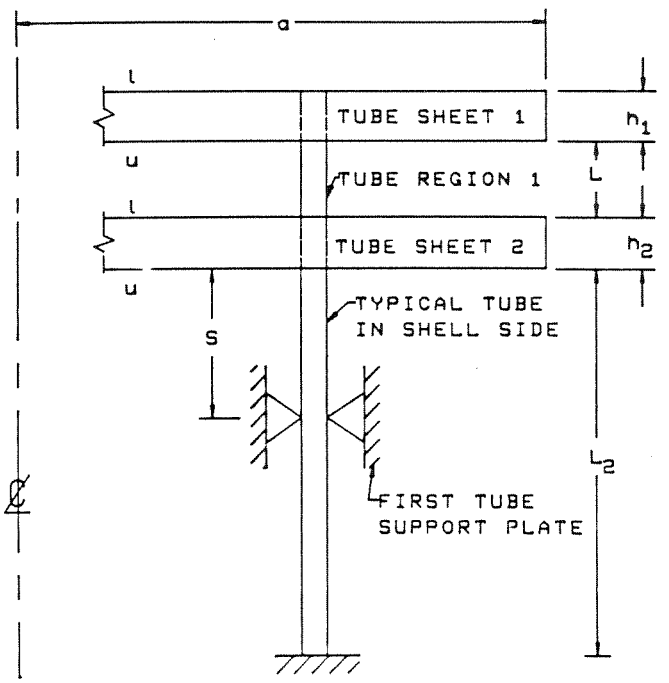


Fig. 1. Double tubesheet configuration.

tubesheets is minimal. Application of the above design formula to set the gap spacing has obvious drawbacks when applied to large units such as central power station condenser tubesheets. Alignment problems may occur in assembly and unit cost can be increased, especially with expensive corrosion-resistant materials, because of the excess tubing required which contributes nothing to heat transfer capacity. It has been suggested[1-3] that the above problems may be relieved by reducing the spacing $L$ between tubesheets to the order of 1 in (2·54 cm) or less. However, as pointed out in reference 3, such a reduction should not routinely be considered unless an appropriate design procedure, which includes all interactions between tubesheets, is applied. In reference 3 the field equations for closely spaced circular tubesheets, which interact because of the tubing, are developed and solved numerically to illustrate the effect of the close spacing. The complex interactions between the tubesheets cause coupling between tubesheet in-plane and out-of-plane deformations and preclude simplified closed form solutions.

In this work we re-examine the closely spaced tubesheet configuration and develop closed form solutions which rival the simplicity of eqn. (1) yet provide a more realistic assessment of interactions between tubesheets and connecting tubes. Anticipating application to large rectangular tubesheets such as are found in central station condensers, we consider the behaviour of two closely spaced plate strips (tubesheets) connected by an elastic foundation (tubes) and subject to in-plane thermal loadings.

Figure 2 shows the double tubesheet configuration to be studied in exploded view so as to exhibit the forces and moments to be considered. The following assumptions are incorporated in the analysis:

(1) Shear deformation is included in the tubing and in both tubesheets.
(2) Thermal loading on each tubesheet is assumed constant through the tubesheet thickness and along the length.
(3) The tubing is assumed stiff enough in axial deformation so that lateral deformation of the tubesheets may be neglected.
(4) Mechanical loading on the tubesheets and tubes is neglected.

We note that the simplifying assumption (3), which suppresses lateral movement of the tubesheets, is conservative insofar as tube design stresses are concerned. Since only thermal stresses are considered, any suppression of structure flexibility tends to predict higher tube stresses in region 1 (see Fig. 1). Thus, results obtained from our efforts, although simple in nature, will be useful in preliminary design studies undertaken to estimate required tubesheet spacing.

## ANALYSIS

Using the notation of Fig. 2, we obtain equilibrium equations for the foundation and for the tubesheets in the form:

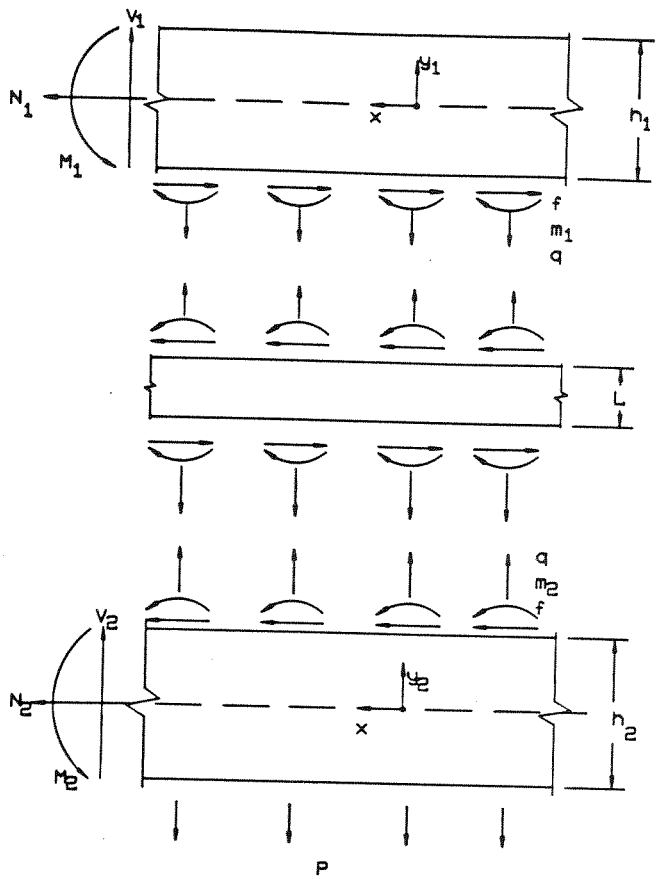


Fig. 2. Free body.

$$m_1 - m_2 + fL = 0 \tag{2}$$

$$\frac{dN_1}{dx} - f = 0; \qquad \frac{dV_1}{dx} - q = 0 \tag{3}$$

$$\frac{dM_1}{dx} + f\frac{h_1}{2} - m_1 = V_1$$

$$\frac{dN_2}{dx} + f = 0; \qquad \frac{dV_2}{dx} = p - q \tag{4}$$

$$\frac{dM_2}{dx} + f\frac{h_2}{2} + m_2 = V_2$$

Constitutive equations for the tubesheet are obtained by using the linear

displacement assumption for each tubesheet in the form ($i = 1, 2$):

$$u_{xi}(x, y_i) = u_i(x) + y_i\theta_i(x) \tag{5}$$
$$u_{yi}(x, y) = u_{zi}(x, y) = 0$$

and by appropriate averaging of the elastic stress–strain relationships through the tubesheet thickness. We obtain relationships for force and moment resultants in the form:

$$N_1 = K_1\left(\frac{du_1}{dx} - \alpha_1 T_1\right); \qquad N_2 = K_2\left(\frac{du_2}{dx} - \alpha_2 T_2\right)$$
$$M_1 = \frac{K_1 h_1^2}{12}\frac{d\theta_1}{dx}; \qquad M_2 = \frac{K_2 h_2^2}{12}\frac{d\theta_2}{dx} \tag{6}$$
$$V_i = \mu G_1 h_1 \theta_1; \qquad V_2 = \mu G_2 h_2 \theta_2$$

where $K_i = E_i h_i/(1 - \nu^2)$ and $\mu = 5/6$.

In the above equations $\alpha_i$, $T_i$ are the coefficients of thermal expansion and temperature change above ambient of the $i$th strip. The material constants are $E_i$, $G_i$, $\nu_i$ and the thickness of each strip is $h_i$. Note that we employ assumption (3) to suppress lateral deformation components that ordinarily appear in the last of eqns. (6).

Assuming that the elastic foundation between the tubesheets is representative of a fully packed tube array, we can show[3,4] that the following equations relate $f$ and $m_i$ to the tubesheet deformation parameters:

$$f = \frac{6K^*}{L}\left(u_D - \frac{h_i}{2}\theta_1 - \frac{h_2}{2}\theta_2\right) \tag{7}$$
$$m_1 = -m_2 - fL/2$$

where:

$$u_D = u_1(x) - u_2(x) \tag{8}$$

and:

$$K^* = \frac{2E_T I_T}{A}\Big/(12g + L^2); \qquad g = \lambda\frac{E_T I_T}{G_T A_T} \tag{9}$$

In eqn. (9), $E_T$, $G_T$, $A_T$, $I_T$ are the tube moduli in tension and shear, and the cross-section metal area and moment of inertia, respectively. $A$ has the dimensions of area and is representative of the repeated drilling pattern of the tubesheet. Figure 3 shows the repeated tube pattern leading to a value of $A$ for a diagonal tube array. For a thin walled tube $\lambda = 2$; for a solid circular bolt, $\lambda = 4/3$.

Adding the first of eqns. (3) and (4) and integrating yields:

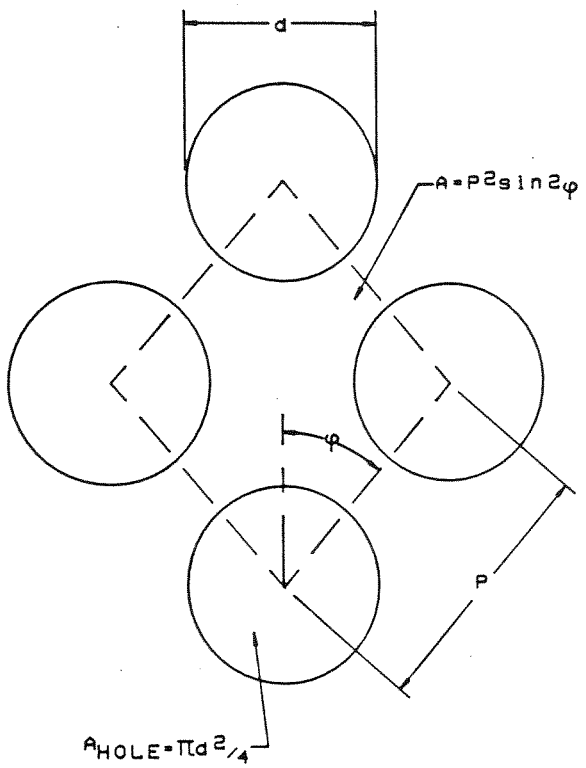


Fig. 3. Diagonal tube array pattern.

$$N_1(x) + N_2(x) = \text{Const.} \tag{10}$$

Under the assumption of zero net in-plane force:

$$N_1(x) = -N_2(x) = P(x) \tag{11}$$

and we may write the necessary field equations for our further perusal in the form:

$$\frac{dP}{dx} = f; \qquad \frac{du_D}{dx} = \frac{(1 + K_1/K_2)}{K_1} P(x) + (\alpha_1 T_1 - \alpha_2 T_2) \tag{12}$$

$$\frac{K_1 h_1^2}{12} \frac{d^2\theta_1}{dx^2} + f \frac{(h_1 + L)}{2} = \mu G_1 h_1 \theta_1 \tag{13}$$

$$\frac{K_2 h_2^2}{12} \frac{d^2\theta_2}{dx^2} + f \frac{(h_2 + L)}{2} = \mu G_2 h_2 \theta_2 \tag{14}$$

Equation (7) provides the necessary relationship between $f(x)$ and the deformation parameters. Associated with the above sixth order system are boundary conditions on $d\theta_1/dx$ or $\theta_1$, $d\theta_2/dx$ or $\theta_2$ and $P(x)$ or $u_D$ at the edges $x = 0, a$.

Equations (7), (12), (13) and (14) are seven equations to solve for the variables $f$, $m_1, m_2, P, u_D, \theta_1$ and $\theta_2$. Of these, we are primarily interested in $f, m_1$ and $m_2$ as these directly relate to the state of stress in the tubes between the tubesheets under the thermal driving 'force' $\alpha_1 T_1 - \alpha_2 T_2$. In the following section we consider further simplifications leading to formulas suitable for preliminary design. With $f, m$ determined, we can establish the following results for tube shear stress, $\tau$, and maximum tube bending stress, $\sigma$:

$$\tau = \alpha f A / A_T; \qquad \sigma = m A d_T / (2 I_T) \tag{15}$$

where $d_T$ is the outer diameter of a tube, $\alpha = 2{\cdot}0$ if $\tau$ represents the magnitude of the maximum shear stress and $\alpha = 1{\cdot}57$ if $\tau$ represents the magnitude of the average shear stress. Note that since $m = Lf/2$ in all of our subsequent work, determination of the maximum value of the shear stress $f(x)$ is sufficient for evaluation of tube stresses. In the numerical computations herein we suggest that if $S_a$ is an allowable design stress for the tube material, then an acceptable design is obtained if $\sigma \leq S_a$ and $\tau \leq S_a/\sqrt{3}$.

## APPROXIMATE SOLUTIONS

### (A) *Tubesheet bending and shear neglected*

The simplest approximation offering any improvement over eqn. (1) is obtained by neglecting bending and shear in the tubesheets. Hence, we consider only eqns. (7) and (12), with $\theta_1 = \theta_2 = 0$, and subject to boundary conditions:

$$u_D(0) = 0; \qquad [P + K_B u_D]_{x=a} = 0 \tag{16}$$

$K_B$ represents the effect of edge restraint provided by flange bolting, etc. In this and subsequent solutions, we consider edge bolt restraint only and use:

$$K_B = \frac{12 E_B I_B / L_B W_B}{(L_B^2 + 12 g_B)}; \qquad g_B = \frac{4}{3} \frac{E_B I_B}{G_B A_B} \tag{17}$$

In the above, $L_B$ is the effective length of bolting and $W_B$ is the spacing between bolt centres along the flange. $E_B, G_B, A_B, I_B$ have the same meaning for the edge bolting as the previously defined quantities for the interior tubing. We note that in this and subsequent analyses, the effect of an untubed periphery around the tubesheets is neglected.

From the above equations we obtain the solution for the maximum foundation surface shearing stress, occurring at $x = a$, as:

$$f(a) = \frac{6K^*}{\beta_1 L} \frac{(\alpha_1 T_1 - \alpha_2 T_2) \tanh \beta_1 a}{\left[1 + \dfrac{K_B(1+\varepsilon)}{\beta_1 K_1} \tanh \beta_1 a\right]} \tag{18}$$

with:

$$\beta_1^2 = \frac{6K^*(1+\varepsilon)}{K_1 L}; \qquad \varepsilon = K_1/K_2$$

If we neglect tubesheet in-plane elasticity (i.e. let $K_1$, $K_2 \to \infty$) then eqn. (17) reduces to:

$$f(a) = \frac{6K^*(\alpha_1 T_1 - \alpha_2 T_2)a}{L} \tag{19}$$

If shear deformation in the tubes is neglected (i.e. set $g = 0$ in eqn. (9) defining $K^*$), then eqn. (19), the second of eqns. (7) and the second of eqns. (15) lead to the result presented as eqn. (1). Hence, the approximate solution given by eqn. (18) represents an improvement over eqn. (19) (and hence eqn. (1)) in that tubesheet edge restraint, in-plane elasticity and tube shear deformation effects are included.

(B) *Tubesheet bending neglected*

In this approximation, we again reduce the system to second order by neglecting terms involving second derivatives in eqns. (13) and (14). This is equivalent to assuming that tubesheet bending moments are negligible. Since eqns. (13) and (14) now yield direct algebraic relations for $\theta_1$, $\theta_2$, subsequent combination with eqns. (7) and (12), together with the boundary conditions of eqn. (16), yields a simple solution for the maximum value of the foundation shear stress $f$ (at $x = a$) as:

$$f(a) = \frac{6K^*}{\beta_2 L(1+\gamma)} \frac{(\alpha_1 T_1 - \alpha_2 T_2)\tanh \beta_2 a}{\left[1 + \dfrac{K_B(1+\varepsilon)}{\beta_2 K_1}\tanh \beta_2 a\right]} \tag{20}$$

where:

$$\gamma = \frac{6K^*}{4\mu L}\left[\frac{h_1 + L}{G_1} + \frac{h_2 + L}{G_2}\right]$$
$$\beta_2^2 = \frac{6(1+\varepsilon)K^*}{K_1 L(1+\gamma)} \tag{21}$$

and the remaining quantities are as defined previously.

(C) *Identical tubesheets*

For the case of identical tubesheets, with boundary conditions the same for both tubesheets, the system of equations reduces to a fourth order system in the variables $u_D$ and $\theta$ where $\theta_1 = \theta_2 = \theta$.

$$\frac{K_1 h^2}{12}\theta'' + \frac{K_1(h+L)}{4}u_D'' - \mu G h\theta = 0$$
$$\frac{K_1 u_D''}{2} = \frac{6K^*}{L}(u_D - h\theta) \tag{22}$$

Boundary conditions are $M_1 = M_2 = M$ or $\theta$ specified at $x = 0, a$; also $P + K_B u_D = 0$ at $x = a$, and $u_D = 0$ at $x = 0$. The solution to the above system is easily obtained and calculations required to determine $f(a)$ are carried out on the computer. We will use the results of this problem to assess the probable accuracy of our previous approximations. It can easily be shown for the case of no gap ($L = 0$) between the tubesheets that:

$$u_D = h\theta \tag{23}$$

and the system again reduces to one of second order satisfying:

$$\theta'' - \beta_3^2\theta = 0; \qquad \beta_3^2 = \frac{3\mu G_1}{K_1 h} \tag{24}$$

with $\theta(0) = 0$; $P + K_B h\theta = 0$ at $x = a$.

For the case of zero gap, we obtain the analogue of eqns. (18) and (20) as:

$$f(a) = \frac{K_1}{2} \frac{\beta_3(\alpha_1 T_1 - \alpha_2 T_2)\tanh \beta_3 a}{\left[\frac{4}{3} + \frac{2K_B}{K_1\beta_3}\tanh \beta_3 a\right]} \tag{25}$$

In closing this section we note that it is a straightforward procedure to solve the full sixth order system. However, since our aim is to develop simple expressions for $f(a)$, such as eqn. (20), we do not choose to pursue this solution. In the next section we show that numerical comparisons of solutions obtained using eqns. (18), (20) and (25) indicate that eqn. (20) is an acceptable approximation for most design computations. If one is interested in a more exact analysis it is best to abandon assumptions (3) and (4) of this paper and attack the full problem numerically following the approach of reference 3.

## NUMERICAL COMPUTATIONS

As an initial application of the developed solutions, we consider tubesheets of equal thickness. The tubesheet properties are:

$$\begin{aligned} &E_1 = E_2 = 30 \times 10^6 \text{ psi } (206{\cdot}8 \times 10^9 \text{ N/m}^2) \\ &h_1 = h_2 = 1{\cdot}75 \text{ in } (4{\cdot}445 \text{ cm}) \end{aligned} \tag{26}$$

and the tube array is assumed diagonal (Fig. 3) with the properties:

$$\begin{aligned} &E_T = 18 \times 10^6 \text{ psi } (124{\cdot}1 \times 10^9 \text{ N/m}^2) \\ &\text{Tube outer diameter } d_T = 1{\cdot}00 \text{ in } (2{\cdot}54 \text{ cm}) \\ &\text{Tube thickness} = 0{\cdot}049 \text{ in } (0{\cdot}1245 \text{ cm}) \\ &\text{Tube pitch } P = 1{\cdot}25 \text{ in } (3{\cdot}175 \text{ cm}); \ \phi = 30^\circ \end{aligned} \tag{27}$$

We assume edge restraint in the form of 1·375 in (3·4925 cm) diameter steel bolts on 4 in (10·16 cm) centre to centre spacing. We assume that the effective elastic length of the bolt $L_B$ is approximated as:

$$L_B = L + \frac{h_1 + h_2}{4} \tag{28}$$

The length of strip $a$, over which unrestrained thermal growth is permitted, is taken in all of the numerical computations to follow as:

$$a = 80 \text{ in } (203{\cdot}2 \text{ cm}) \tag{29}$$

The effective elastic constants for the tubesheet, which account for the weakening effect of the perforations, are obtained by applying the formulae in reference 5.

The above configuration is used in the input to a computer program which performs the necessary algebraic computations for approximations (A) and (B) discussed in the previous section. For the special case of equal tubesheets, the computer program also develops the solution for the approximation (C) for gap spacing greater than or equal to zero. Figure 4 shows the results obtained for the allowable thermal loading parameter:

$$\Delta_T = |\alpha_1 T_1 - \alpha_2 T_2| \tag{30}$$

as a function of the dimensionless gap spacing $L/L_0$ where $L_0 = 10$ in (25·4 cm). For the configuration under analysis, eqn. (15) is used where applicable with an allowable design stress $S_a$ taken as:

$$S_a = 7500 \text{ psi } (5{\cdot}17 \times 10^6 \text{ N/m}^2) \tag{31}$$

Also plotted in Fig. 4 is the approximate solution suggested by eqn. (1).

The results summarised in Fig. 4 indicate that case (A) yields a conservative result for all gap spacings, case (B) yields a more acceptable result and that we can probably obtain useful results from case (B) in the region below $L/L_0 < 0{\cdot}5$ by projecting the tangent to the curve at $L/L_0 = 0{\cdot}5$ back to the vertical axis. Similar behaviour has been obtained for other equal tubesheet configurations with a wide variety of tube, tubesheet material properties and geometry. It is concluded that for the configuration reported on here there exists a 'pocket' in the range of gaps:

$$0{\cdot}075 < L/L_0 < 0{\cdot}225 \tag{32}$$

where a thermal load $\Delta_T$ can be tolerated that is equal to or greater than the tolerable thermal loading at $L/L_0 = 0{\cdot}7$. As expected, the predictions of eqn. (1) are extremely conservative and imply that a large gap spacing is required for successful operation.

We now consider the application of the case (B) approximation to some practical configurations having different shell side and tube side tubesheet geometries and/or material properties. We emphasise in these subsequent results the effect of edge restraint and the effect of different tubesheet thickness on the permissible thermal

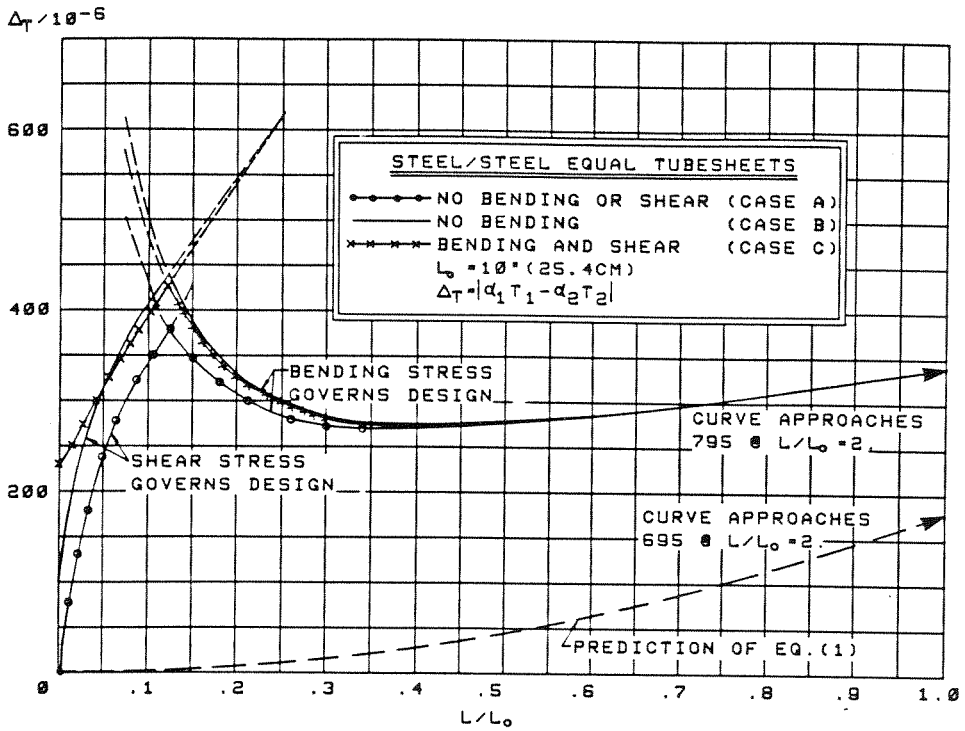


Fig. 4. Comparison study of different approximations for equal tubesheets.

loading $\Delta_T$. Figure 5 shows results obtained for the tubesheet combination:

$$E_1 = E_2 = 30 \times 10^6 \text{ psi } (206{\cdot}8 \times 10^9 \text{ N/m}^2)$$
$$h_1 = 1 \text{ in } (2{\cdot}54 \text{ cm}) \qquad h_2 = 0{\cdot}5 \text{ in } (1{\cdot}27 \text{ cm}) \tag{33}$$

The tube array is 60° diagonal with every fourth row of tubes removed. This array is denoted as a 'laned' array in reference 5 and is used to promote steam flow to the interior of the tube bundle. The appropriate formulas for calculating effective elastic constants and area factor $A$ (in eqn. (9)) are found in that reference. The tube material and geometric properties are:

$E_T = 30 \times 10^6$ psi $(206{\cdot}8 \times 10^9$ N/m$^2)$
Tube outer diameter $d_T = 1{\cdot}0$ in (2·54 cm)
tube thickness 0·028 in (0·071 cm)
Tube pitch = 1·25 in (3·175 cm) (used in computing effective properties in accordance with reference 5) (34)
Allowable stress $S_a = 20{,}000$ psi $(137{\cdot}9 \times 10^6$ N/m$^2)$

Two different edge restraints are studied using steel bolts:

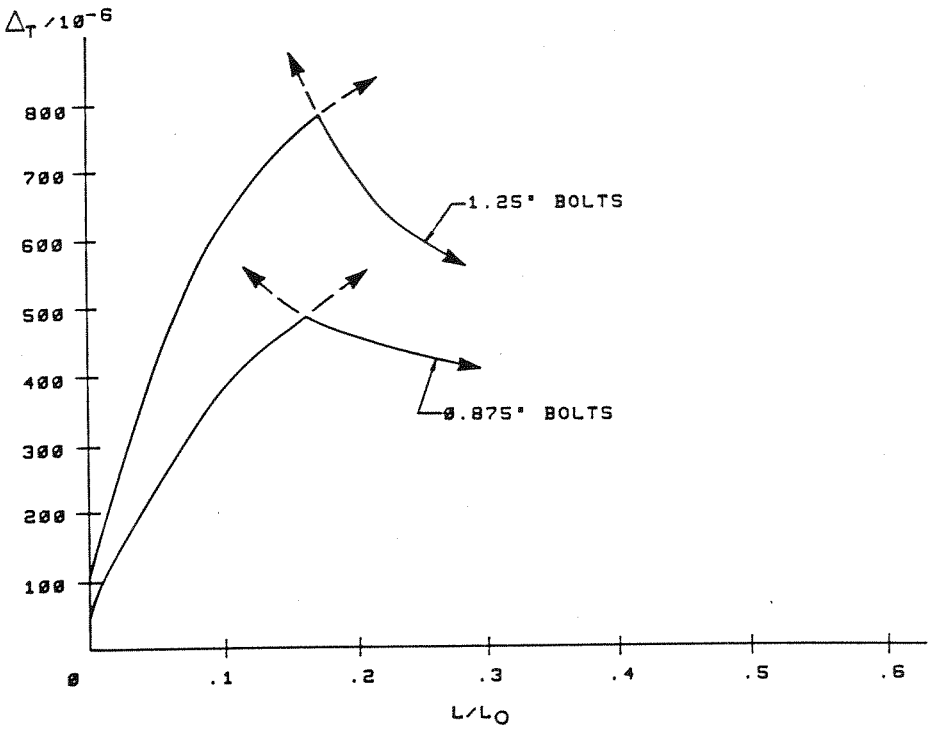


Fig. 5. Design results showing effect of edge restraint.

0·875 in (2·2225 cm) diameter on 4 in (10·16 cm) spacing (35)
1·250 in (3·175 cm) diameter on 3 in (7·62 cm) spacing

For this study $L_B$ is taken as the distance between tubesheet centrelines and the length of strip $a$ is the same as in the previous study. The results shown in Fig. 5 clearly illustrate that increasing edge restraint yields a higher allowable $\Delta_T$ for the entire range of gap distances. It is clear that increased edge restraint, although decreasing the tube stress, increases the direct stress in each tubesheet; in an actual application the user must be aware of the interaction between tubes and tubesheet and design accordingly.

Figure 6 shows results obtained for a third study in which emphasis is placed on the effect of thickness changes in the shell side tubesheets. The tubesheet configuration for this investigation is:

$$E_1 = 17 \times 10^6 \text{ psi } (117{\cdot}19 \times 10^9 \text{ N/m}^2);\ h_1 = 1{\cdot}0 \text{ in } (2{\cdot}54 \text{ cm})$$
$$E_2 = 30 \times 10^6 \text{ psi } (206{\cdot}8 \times 10^9 \text{ N/m}^2)$$
$$h_2 = 1{\cdot}0 \text{ in } (2{\cdot}54 \text{ cm}) \quad \text{or } h_2 = 0{\cdot}625 \text{ in } (1{\cdot}588 \text{ cm}) \tag{36}$$

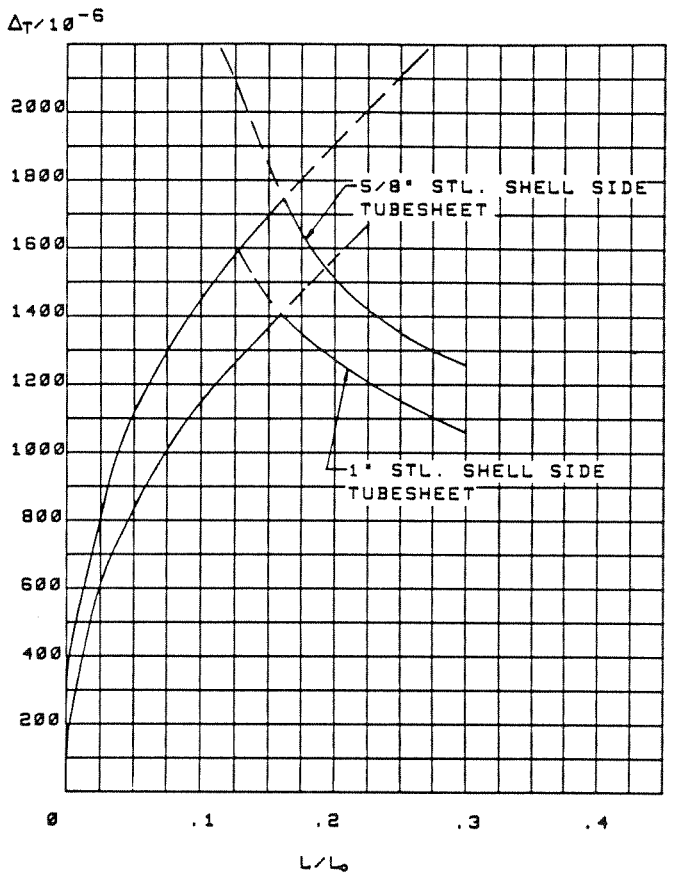


Fig. 6. Design results showing effect of varying tubesheet thickness.

The tube material is titanium, $E_T = 15 \times 10^6$ psi ($103{\cdot}4 \times 10^9$ N/m$^2$) with allowable design stress assumed as $S_a = 26{,}600$ psi ($183{\cdot}4 \times 10^6$ N/m$^2$). The rest of the tube dimensions are the same as in the previous study. The edge restraint for this problem consisted of 1·25 in (3·75 cm) diameter steel bolts on 3 in (7·62 cm) spacing. The remaining geometry is the same as previously considered. Figure 6 indicates that the thinner shell side tubesheet permits a higher allowable $\Delta_T$. As before, the effect on the tubesheet direct stress must be considered in the application but is not reported on herein.

## SUMMARY

In the preceding work we have presented a series of approximate solutions leading to predictions of the maximum allowable differential in-plane movement of tubesheets

in a double tubesheet configuration due to thermal loading. The solutions obtained emphasise the interaction between tubesheet spacing, tubing between the tubesheets, tubesheet elasticity and edge restraint. We show that the effect of tube shear deformation must be included in order to obtain realistic results. We conclude that it is possible to design closely spaced double tubesheet configurations in the presence of differential thermal loading of the tubesheets. It is important to recognise that for small tubesheet spacing, tube shear effects predominate, while for moderate and large gaps tube bending predominates. The approximate solution which neglects tube shear, tubesheet elasticity and edge restraint yields overly conservative results which preclude the employment of double tubesheet configurations.

## REFERENCES

1. YOKALL, S., Double tubesheet heat exchanger design stops shell tube leakage, *Chemical Engineering* (May, 1973), pp. 133–6.
2. PEAKE, C. C., GERSTENKORN, G. F. and ARNOLD, T. R. Some reliability considerations—Large surface condensers, Paper presented to *American Power Conference*, Chicago, Ill., April, 1975.
3. SOLER, A. I., Analysis of closely spaced double tubesheets under mechanical and thermal loadings, ASME Paper 77JPGC-NE-21, *Joint Power Generation Conference*, Long Beach, California, Sept., 1977.
4. COOK, R. D., *Concepts and applications of finite element analysis*, J. Wiley, New York, 1974, p. 333.
5. SOLER, A. I. and HILL, W., Effective elastic constants for large condenser tubesheets, *ASME Journal for Power*, **99**(3) (July, 1977), pp. 365–70.